Reducing Grid Distortions Utilizing Energy Demand Prediction and Local Storages

PASCAL A. SCHIRMER[ID][1], **CHRISTIAN GEIGER**[ID][2], **AND IOSIF MPORAS**[ID][1]

[1]School of Engineering and Computer Science, University of Hertfordshire, Hatfield AL10 9AB, U.K.
[2]Institute for Machine Tools and Industrial Management, Technical University of Munich, 85748 Garching, Germany

Corresponding author: Pascal A. Schirmer (p.schirmer@herts.ac.uk)

ABSTRACT Energy storage systems will play a key role in the establishment of future smart grids. Specifically, the integration of storages into the grid architecture serves several purposes, including the handling of the statistical variation of energy supply through increasing usage of renewable energy sources as well as the optimization of the daily energy usage through load scheduling. This article is focusing on the reduction of the grid distortions using non-linear convex optimization. In detail an analytic storage model is used in combination with a load forecasting technique based on socio-economic information of a community of households. It is shown that the proposed load forecasting technique leads to significantly reduced forecasting errors (relative reductions up-to 14.2%), while the proposed storage optimization based on non-linear convex optimizations leads to 12.9% reductions in terms of peak to average values for ideal storages and 9.9% for storages with consideration of losses respectively. Furthermore, it was shown that the largest improvements can be made when storages are utilized for a community of households with a storage size of 4.6-8.2 kWh per household showing the effectiveness of shared storages as well as load forecasting for a community of households.

INDEX TERMS Load prediction, grid distortion, local storages, non-linear optimization.

I. INTRODUCTION

Global average temperatures are rising due to the increasing amount of greenhouse gas emissions causing natural disasters and having negative impact to nature and humans [1]. As currently the largest share of CO_2 emissions are caused by burning of fossil fuels, renewable energy sources are increasingly employed in order to reduce the carbon footprint of the primary energy sector [2]. However, with the integration of increasing amounts of renewable energy, the supply of energy is stronger varying due to the external dependencies of renewable energies, i.e. wind or sunshine [3]. Therefore, to account for the increasing volatility of energy generation, combined with the volatility of energy demand, three major topics have been addressed in literature in order to reduce grid distortions and peak loads, namely load prediction, integration of storages and demand management [1], [4]. Especially, when considering storage optimizations or advanced demand management usually a load prediction architecture is combined with a shared storage unit in order to find optimal charging/discharging strategies under certain constraints.

The associate editor coordinating the review of this manuscript and approving it for publication was Fabio Massaro[ID].

Therefore, in the following chapters a detailed literature review of load prediction, integration of electrical storages and demand management is provided.

As regards load prediction it is a time series prediction problem [4], [5]. Data can be collected from smart-meters, usually one per customer, which in most cases is equivalent to one per household. The energy consumption data, which are usually collected with sampling period from one second to one hour, in most cases consist of active power samples and less often reactive power, load angle and current harmonics [6], [7]. For the residential sector the interest is mostly in short-term predictions (sub-hourly, hourly) for the prevention of blackouts, but also in long-term predictions (monthly, yearly) for national planning and investment [8], [9]. The prediction of energy consumption is a difficult task, because except the periodic patterns (e.g. daily and weekly routines) irregular components appear in the energy consumption signal as well [10]. Energy prediction has been utilized to predict the consumption of households and buildings. Two main approaches have been investigated, namely the physical modelling and the data-driven approaches. The physical models are based on thermodynamic coupling for precise energy analysis and use parameters such as building

construction details, operation schedules, climate characteristics, etc. [1], [5]. Due to the high number of parameters and the complex interactions, an accurate estimation of the energy consumption is intrinsically difficult. Conversely, data driven models use recorded data and try to predict the demand based on past energy consumption patterns. The data driven methods have the advantage of faster calculation, while being suitable for non-linear modelling [1]. Since the prediction of energy consumption is a difficult task due to the irregular components appearing in the energy consumption signal [10], several different methods for improving the load prediction accuracy have been proposed. Several different machine learning classifiers have been evaluated, namely Linear Regression (*LR*) [10], Support Vector Regression (*SVR*) [11], Decision Trees (*DTs*) [10] and deep learning methods like Convolutional Neural Networks (*CNNs*) [12], Recurrent Neural Networks (*RNNs*) [10] and Long Short Term Memory (*LSTM*) [12]. Furthermore, additional input features like temperature, humidity, radiation etc., have been used to improve prediction accuracy [8], [9]. In detail, the approach presented in [10] focuses on the different effects of the calendar, i.e. seasonal and weekly effects, while providing insights on the effect of different granularities of the output of the prediction model. This comes with the advantage of having a predictor that can possibly work with a lower data granularity (sampling frequency), but might lead to forecasting errors for transient events if the sampling period exceeds a certain limit. Furthermore, the approach presented in [12] evaluates especially high resolution data (1/60 Hz) for spatial and temporal resolution by combining a CNN and LSTM based model in order to capture periodic as well as irregular patterns. This comes, conversely to [10], with the advantage of capturing very accurately transient responses due to the spatial and temporal coverage of the model, however requires a by far more complex, multi-dimensional CNN-LSTM architectures.

Storage systems have been integrated into households and buildings in order to have an additional degree of freedom in load management. Different storage types, namely hydrogen storages [13], thermal storages with integrated gas and district heating [14], as well as power to gas technologies [15], have been studied in terms of their integration into microgrids as well as their application for demand management systems. Both optimizations for consumer households and utility companies have been proposed [16]. Storage systems enable consumer households to store electrical energy during times of low demand at which electricity price is low, while consuming or selling it back to the network during peak hours, thus reducing energy cost [17], [18]. However, this could possibly lead to sudden peak demands during low pricing periods and thus multiple regulations in terms of dynamic pricing by the utility grid operator. Therefore, for utility companies storage systems can be used to de-couple the energy production from the demand. Therefore, the generating capacity of power plants will match the average electrical demand instead of the peak demand as discussed in [19]. Demand Side Management (DSM) has been implemented utilizing both load

prediction and storage systems. Specifically, a dynamic game theory approach for DSM considering forecasting errors was presented in [16], with optimal battery sizing and advanced battery modelling discussed in [1] and [20]. This approach has the advantage of considering forecasting errors, utilizing and accurate battery model with loss modelling and using a quadratic cost function for energy pricing, however it does not consider any methods for reduction of forecasting errors as well as it does not consider grid distortion minimization as an objective in the cost function. Feature extraction and feature ranking for accurate load prediction and load modelling were evaluated in [21]. Furthermore, several optimization approaches for cost minimization have been proposed within microgrid structures, like model predictive control which was used in [22] to reduce energy bills an accurately model the degradation cost of the storage, while in [23] an offline optimization for cost optimization was presented under the assumption of zero forecasting errors. Especially in [22] the advantage is the high power of model predictive control, which however has the restriction of high computational cost for long prediction horizons, while in [23] the modelling without forecasting errors is a significant downside. Moreover, load prediction and optimization architectures using photovoltaic generation and battery powered vehicles have been presented in [24]–[26] and [27]–[29] respectively. Additionally, combined approaches for smart homes including photovoltaic energy generation and storages as well as demand management have been proposed [30]–[32]. Moreover, next to economic optimization constraints different optimization approaches for demand management and demand response have been proposed with optimization of thermal comfort having a large share of these additional constraints. Especially, thermal comfort was optimized under the consideration of electricity generation through photovoltaic in [33] and under consideration of occupancy in households [34]. Latest approaches have been focusing on multi-carrier energy systems as well as virtual energy hubs, thus considering the physical structure of a microgrid with several energy sources, e.g. thermal storages, electrical storages, power-to-gas, etc., and several consumers. In detail, economic optimizations considering energy pricing have been considered for power to gas technology with shiftable loads in [15], for a coalition of several home energy hubs with a heuristic bidding strategy in [35], for a community of households with storage as well as electrical and thermal energy generator in [36] and for a self-organized multi carrier energy system trying to optimize its revenue across different local energy markets in [37].

The contribution of the proposed approach is twofold and is mainly based on utilizing one common storage for a community of households while additional information of this community is utilized to improve the load predictor and the storage optimization. First, the accuracy of the load prediction stage is improved through utilization of inter-household dependencies, i.e. similar energy consumption patterns in neighbouring households, and socio-economic information, i.e. the size of the property or the age of the residents.

To the best of the authors knowledge the utilization of socio-economic features was not presented previously in the literature. However, as real world implementations of a storage optimization procedure mostly rely on ahead predictions of the load demand [16], having an accurate load predictor is crucial for applying a storage optimization strategy. Second, whereas previous publications have focused strongly on reducing cost or energy consumption when utilizing a storage with a demand management system [22]–[24], thus focusing on the consumer side, the proposed approach focuses on minimizing the grid distortions and thus the generation side. This is of importance as with rising proportion of renewable energies high variances appearing not only on the demand side but also on the generation side. Therefore, it is beneficial to utilize energy storages in order to reduce the variance of consumer demand, thus making consumer household constant loads which are not varying over time [24]. Especially, having consumer households with constant consumption over time would be advantageous for the grid operator due to the possibility of better planning and focusing on the variance of the energy generation, i.e. modelling the statistical variance of the renewable energy sources. The proposed solution is presented as non-linear optimization problem in closed form under consideration of an advanced storage model similarly to [20].

The remainder of this article is organized as follows: Section II gives a short introduction to the proposed architecture. In Section III the load management strategy is presented. In Section IV the experimental setup is described and in Section V the evaluation results are presented. Finally, discussions and conclusions are provided in Section VI and Section VII respectively.

II. SYSTEM MODEL

As conventional grid structures do not include storages and thus are not able to buffer fluctuations of energy demand or supply, conventional energy generation units are designed to operate at low variance delivering energy according to the demand. However, with the integration of renewable energy sources in the grid the variance of the energy supply is increasing as illustrated in Fig. 1.

As can be seen in Fig. 1a the energy demand of consumers and industry underlies a high variance due to microscopic events (e.g. load changes caused by daily or weekly activities, i.e. day/night patterns or weekdays and weekends) and macroscopic demand changes (e.g. increased demand during winter times due to additional heating). These demand variances were previously buffered by conventional power plants generating energy according to the demand with very low variance, e.g. through burning of fossil fuels (Fig. 1b) [3]. However, as this will not be possible with renewable energies (e.g. wind or photovoltaic), due to their volatile behaviour as illustrated in Fig. 1c, local storages have been proposed as energy buffers reducing the variance at the demand side [1]. The architecture considered in this article consists of a utility company (Section II-A) providing energy to a community of
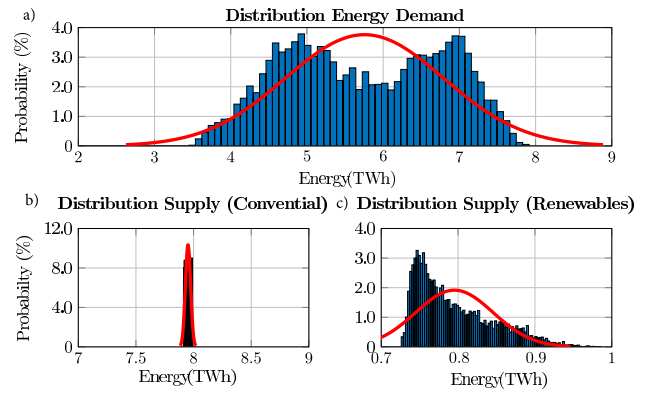

FIGURE 1. Histogram of the energy demand and supply distribution including estimates of the normal distributions (red line) in Germany in 2014 [3]. Specifically, sub-figure a) illustrates the energy demand while sub-figure b) and c) illustrate the energy generation for conventional and renewable energy sources respectively.
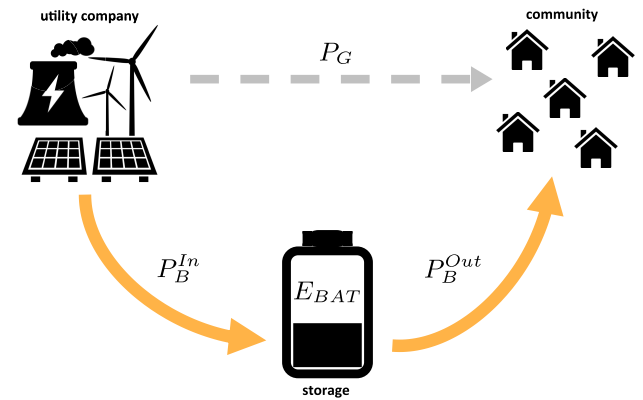

FIGURE 2. Proposed smart grid architecture, adapted from [1], including a utility company for energy generation (might include conventional or renewable energy generation), a community of consumer households sharing one common battery storage [1]. Energy might flow directly from the utility company to the consumer household (P_G) or be stored intermediate in the storage (P_B^{In}).

households (Section II-B) and a local storage (Section II-C) as illustrated in Fig. 2.

In detail, as illustrated in Fig. 2 the proposed high-level architecture consists of a utility company distributing the electrical energy to a consumers community via a grid. Additionally, to transferring the energy via the conventional grid there is the possibility to intermediately store it into an energy storage. In this architecture the power balance constraint is formulated as:

$$P_L(t) = P_G(t) + P_B(t) \qquad (1)$$

where $P_L(t)$ is the aggregated load demand of the community, $P_G(t)$ the power transferred via the grid and $P_B(t)$ the charging ($P_B^{In}(t)$) or discharging ($P_B^{Out}(t)$) power of the battery. Detailed models for the utility company, the grid and the community are provided in Sections II-A,B,C.

A. UTILITY COMPANY

The utility company is providing energy to the community of households via a grid, $P_G(t) \ \forall t : t \in \{1, \dots, T\}$, for each

time step t. For the modelling of the utility company and the grid the following assumptions have been made:

1) The generation capacity of the utility company is infinite, thus it can always provide the demanded energy.
2) The grid has ideal/lossless behaviour.
3) The response to load changes is instant, thus no transients, i.e. changes in grid frequency, appear.
4) External weather conditions, i.e. sunshine, wind or rain, are not explicitly considered by the model.

B. COMMUNITY MODEL

The community consists of M households each of them consuming power $p_m(t) \forall t : t \in \{1, \ldots, T\}$, with $1 \leq m \leq M$, for each time interval t as measured by a smart meter. Specifically the aggregated load $P_L(t)$ and the average aggregated load $\overline{P}_L(t)$ consumed by the community will be:

$$P_L(t) = \sum_{m=1}^{M} p_m(t) \tag{2}$$

$$\overline{P}_L(t) = \frac{1}{T} \sum_{T} P(t) \tag{3}$$

A typical example of daily energy demand of the community is illustrated in Fig. 3.
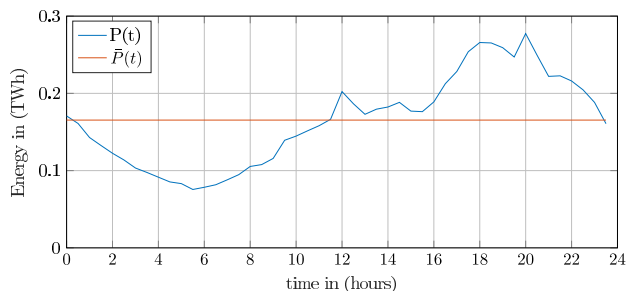
FIGURE 3. Hourly ($P(t)$) and average ($\overline{P}(t)$) load demand for one day of a community of consumer households from the Smart Meters in London database.

As shown in Fig. 3 the load demand of the community is strongly time varying during the day following the solar cycle with a constant time shift of roughly 6h, with high demands during the evening hours and low demand during the night.

C. STORAGE MODEL

A battery model considering charging/discharging efficiency, ageing and self-discharging was developed in order to get a realistic representation of a community storage used for load scheduling. Specifically, Constant-Current-Constant-Voltage (CC/CV) charging was implemented as it is the most common charging principle [38]. The charging and discharging behaviours are illustrated in Fig. 4.

In detail, in Fig. 4 the charging and discharging behaviour are illustrated for current, voltage and State of Charge (SOC). Specifically, the battery is charged with a constant current until charging capacity C^* is reached, while for capacities
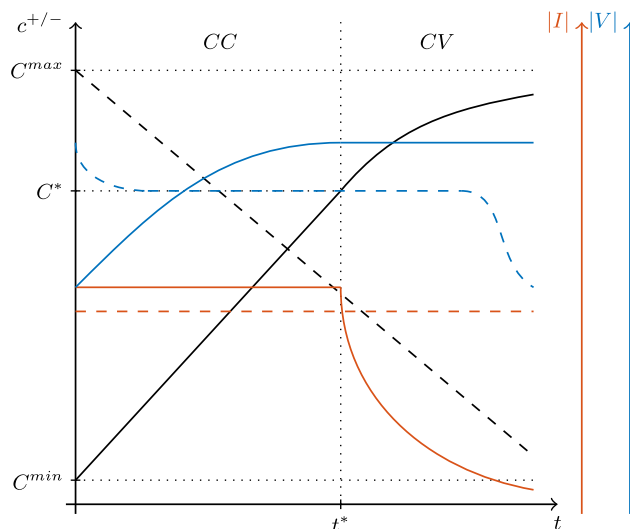
FIGURE 4. Schematic illustration of the charging and discharging behaviour of a lithium-ion battery (solid: charging; dashed: discharging). Black lines denote state of charge, while red and blue lines denote current flowing out of the battery cell and voltage at the terminals respectively.

$C > C^*$ constant voltage is applied for the charging process. Therefore, for SOCs $C > C^*$ the charging power is slowly reduced and if a certain charging current is undercut, the charging process is stopped [39]. In Eq. 4 the charging behaviour for an incremental time step is described for the CC and CV phase respectively [39]:

$$\frac{dC^+}{dt} = \begin{cases} \eta^+ \cdot I_C = const, & t \in CC \\ \eta^+ \cdot c_{max} \cdot \gamma_1 \cdot e^{-\frac{t-t^*}{\gamma_2}}, & t \in CV \end{cases} \tag{4}$$

where C^+ is the stored energy during charging, η^+ is the charging efficiency, I_C the charging current, c_{max} the maximum capacity of the battery, and γ_1 and γ_2 are parameters which are chosen such that the charging curve is continuous at $t = t^*$. During the discharge process the battery is loaded with a constant current until a certain voltage is reached and the discharging process is stopped. In Fig. 4 the dotted lines represent the case of discharging. The current is constant over the complete SOC range. In detail the SOC is reduced linearly and the voltage is dropping at the beginning and at the end, while being nearly constant in between. The discharge behaviour is described in Eq. 5 as formulated in [39].

$$\frac{dC^-}{dt} = \frac{1}{\eta^-} \cdot I_D \quad \forall C^- \geq c_{min} \tag{5}$$

where C^- is the stored energy in the battery during discharging, η^- is the discharge efficiency, I_D the discharge current and c_{min} the minimum stored energy in the battery. Furthermore, internal short circuits and chemical reactions result in a self-discharge of the battery [40]. For the self-discharge of the battery a model as in [20] has been used:

$$\frac{dC^-}{dt} = (1 - \lambda)^t \tag{6}$$

where t is the total passed time and λ is the self-discharge rate respectively. Moreover, the cyclic battery ageing/degradation represents the capacity fade which occurs while the battery is charged or discharged. For example, during charging at low temperatures it can appear, that the Lithium-Ions do not intercalate correctly, and metallic Lithium is deposited on the electrode surface, which leads to a reduction in capacity [41]. The cyclic capacity fade ΔC is described in [42] and formulated in Eq. 7

$$\Delta C = \mu_C \cdot \int I \, dt \qquad (7)$$

where μ_C is the fading constant and $I = |I_{C/D}|$ is the absolute value of the charging and discharging current, thus $\int I \, dt$ being the total processed energy (Ah) of the storage. Accordingly in the proposed storage model Eq. 7 is used to model the degradation.

III. LOAD MANAGEMENT

As discussed in Section II-B the load demand of the community $P_L(t)$ and thus the grid load $P_G(t)$ is strongly fluctuating over time. As load fluctuations are in general undesirable, due to higher load on the grid and increased control actions of the utility company [16], an optimized storage usage strategy is presented. In detail, an optimization of the storage requires predictions of future energy consumption values, thus a load prediction architecture is introduced in Section III-A, while the storage optimization based on constraint non-linear programming is presented in Section III-B.

A. LOAD PREDICTION

The prediction of an energy consumption of the w^{th}-step ahead prediction of a target house m of the community can be formalized as:

$$\hat{p}_m(t + w) = f_\theta(p_m(t_0 : t)) \qquad (8)$$

where $[t_0 : t]$ is the previous time interval used to predict the wth sample at $(t + w)$, $p_m(t_0 : t) \in \mathbb{R}^{(t - t_0 + 1)}$ is the energy consumption of the previous time window, $\hat{p}_m(t+w) \in \mathbb{R}^1$ its step-ahead prediction of the wth sample and $f(\cdot)$ a regression model (e.g. LR, SVR, LSTM, etc.) with a set of free parameters θ.

We expect that across different households in the community there are common energy consumption trends and motifs, as well as interdependencies due to potential socio-economic similarities or in between them relationships, which potentially have time lags between them or appear simultaneously [22]. This motivates us to use the energy consumption history of $M - 1$ other households as an additional input of information to enhance the prediction of energy load demand of the target house, similarly to the architecture we proposed in [43]. In that case the formalization of the problem is expressed as:

$$\hat{p}_m(t + w) = f_\theta(p_m(t_0 : t), p_{m+1}(t_0 : t))$$
$$with \quad 1 \le m < (M - 1) \qquad (9)$$

with $p_m(t_0 : t)$ being the energy consumption signal in the time window $[t_0 : t]$ for the mth neighboring household of the community. Given that prediction models are trained from several households' data, the use of socio-economic information of the consumers of the target house would result in load demand forecasting models adapted to the characteristics of each socio-economic group of consumers. Socio-economic dependent models are expected to predict more precisely the energy consumption behaviour of a house [21], [43] and the prediction can be formalized as:

$$\hat{p}_m(t + w) = f_\theta(p_m(t_0 : t), p_{m+1}(t_0 : t), s_m)$$
$$with \quad 1 \le m < (M - 1) \qquad (10)$$

where $s_m \in R^K$ is the K-dimensional socio-economic information of the target house. The described architecture using inter-household energy data and socio-economic information for prediction of energy consumption using a regression model is shown in Fig. 5.
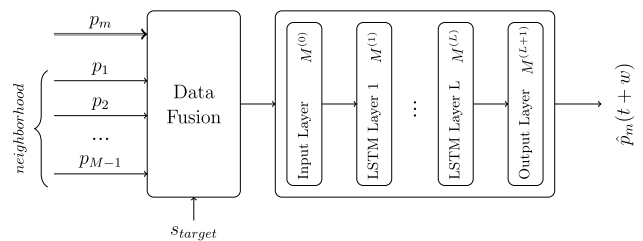

FIGURE 5. LSTM architecture, including the data fusion stage as well as the neural network layout, for energy consumption prediction for the mth household out of a set of M households. Inter-household energy data as well as socio-economic information have been considered.

As can be seen in Fig. 5 the proposed load prediction architecture consists of the data fusion stage, using the energy consumption signals of the different houses and the socio-economic information of each household, and the regression stage providing predictions for the target house $\hat{p}_m(t + w)$. For the regression stage LSTM was chosen as it was found to outperform LR, DTs, DNNs and RNNs on a similar architecture [44]. Furthermore, it must be noted that conversely to [44] the seq2point learning was used instead of seq2seq learning and each time ahead prediction was calculated separately similar as in [16].

B. STORAGE OPTIMIZATION

Let $P = [p(i), p(i+1), \ldots, p(i+W)]$ be a frame of power consumption of length W, $P \in \mathbb{R}_+^W$, where $p(i)$ is the ith sample of P_L and let $\overline{P}$ be the mean value of that frame. Furthermore, let $P_B = [p_B(i), p_B(i + 1), \ldots, p_B(i + W)]$ be a frame of length W, $P_B \in \mathbb{R}^W$, describing the charging and discharging behaviour of the storage. Let $g(\cdot)$ be a cost function considering the cost of employing frame P_B as a charging/discharging strategy. In detail, each sample in frame P_B is optimized in such a way, that it reduces the grid fluctuation and

minimizes Eq. 11.

$$g = \sum_W \left\| \begin{pmatrix} \bar{P}_L \\ \vdots \\ \bar{P}_L \end{pmatrix} - \left[\begin{pmatrix} P(i) \\ \vdots \\ P(i+W) \end{pmatrix} + \begin{pmatrix} P_B(i) \\ \vdots \\ P_B(i+W) \end{pmatrix} \right] \right\|_2 \tag{11}$$

where $\|\cdot\|_2$ is the second norm. As can be seen in Eq. 11 the cost function $g(\cdot)$ depends on the optimization criteria, namely the average power demand of the community $\bar{P}_L$, the instantaneous load demand P and the optimized charging/discharging strategy P_B. In detail optimizing the charging/discharging strategy without any further constraints can be formalized as in Eq. 12:

$$P_B = \underset{P_B \in \mathbb{R}}{\arg\min} \; g(P_B, \bar{P}_L, P) \tag{12}$$

The solution for optimizing $g(\cdot)$ without any restrictions on Eq. 12 is shown in Fig. 6a for one frame of power consumption. In detail the solutions for one frame P are plotted, namely the grid power P_G, the charging strategy of the battery P_B and the capacity C. As illustrated in Fig. 6a an optimization of Eq. 12 might violate the condition $C > 0$. As the storage capacity cannot be negative some restrictions need to be put on Eq. 12, thus Eq. 12 is modified as illustrated in Eq. 13:

$$P_B = \underset{P_B \in \mathbb{R}}{\arg\min} \; g(P_B, \bar{P}_L, P)$$
$$s.t. \; 0 \leq C \leq c_{max} \tag{13}$$

The solution for solving Eq. 13 is illustrated in Fig. 6b for P_G, P_B and C respectively, meeting the restrictions on a finite storage capacity. However, investigating the grid power P_G large distortions appear, as the storage capacity is not optimally scheduled. Therefore, additional constraints need to be put on Eq. 13 in order to reduce the grid distortions.

$$P_B = \underset{P_B \in \mathbb{R}}{\arg\min} \; g(P_B, \bar{P}_L, P)$$
$$s.t. \; Var(P + P_B) = 0$$
$$s.t. \; 0 \leq C_{init} + A \cdot P_B \leq C_{max} \tag{14}$$

where $C_{init} \in \mathbb{R}^W$, $C_{max} \in \mathbb{R}^W$ and $0 \in \mathbb{R}^W$ are vectors of the initial and maximum storage capacities c_{init} and c_{max} as well as the zero vector, while $A \in \mathbb{R}^{W \times W}$ is a quadratic lower triangular matrix with unity elements. In detail, the first constraint of Eq. 14 ($Var(P + P_B) = 0$) ensures that the grid fluctuations are minimal thus reducing the distortions caused by the changing demands of the households, while the second constraint of Eq. 14 ($0 \leq C_{init} + A \cdot P_B \leq C_{max}$) ensures that the capacity of the storage are within the defined minimum and maximum boundaries. In order to turn Eq. 14 into a convex optimization problem with the non-linear constraint of having zero variance of the grid load ($Var(P + P_B) = 0$), Eq. 14 is reformulated as in Eq. 15.

$$P_B = \underset{P_B \in \mathbb{R}}{\arg\min} \; g(P_B, \bar{P}_L, P)$$
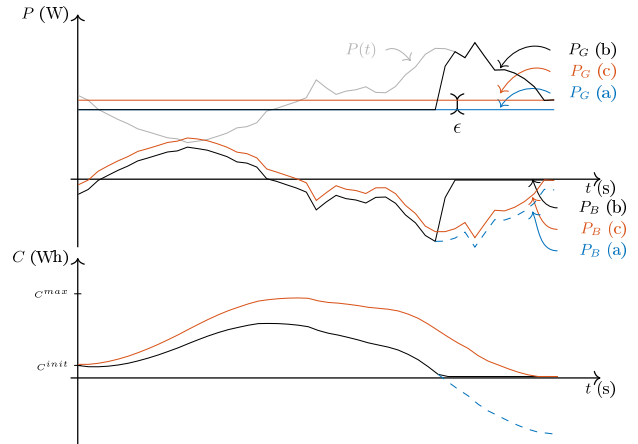$$s.t. \; Var(P + P_B) = 0$$

FIGURE 6. Storage optimization using cost function optimization under certain constraints: a) without constraints, b) with finite storage capacity c) with the proposed optimal load scheduling.

$$s.t. \; C_{init} + A \cdot P_B \leq C_{max}$$
$$s.t. \; -(C_{init} + A \cdot P_B) \leq 0 \tag{15}$$

where the second constraint of Eq. 14 is split into two convex constraints making it solvable with standard solvers. The solution for the optimized operational strategy is illustrated in Fig. 6c.

In detail, Fig. 6 illustrates an example for the load conditions of one day, including the load demand $P(t)$, the grid load P_G and battery charging/discharging P_B for three different constraints as well as the SOC of the storage. As illustrated in Fig. 6 the optimization in Eq. 15 leads to an optimal solution of the storage capacity for a frame of power consumption P. The grid load P_G is reduced to its optimal value, $P_G(t) = \bar{P}_L + \varepsilon \; \forall t \in \{i, \ldots, i+W\}$, being constant for all samples of frame P, where ε is an error term depending on the initial conditions of the storage c^{init} and the maximum storage capacity c^{max}.

IV. EXPERIMENTAL SETUP

The architecture of the system model presented in Section II and the optimized load management including load prediction and storage optimization presented in Section III were evaluated using the dataset, parametrizations and experimental protocols presented below.

A. DATASET

To evaluate the proposed architecture the publicly available dataset "Smart Meters in London" (SMinL) [45] was used. The dataset consists of a re-factored version of the London data store containing the energy readings from 5567 households in London measured between November 2011 and February 2014 at a sampling rate of 1 sample per 30 min. In addition, the dataset contains annotations regarding the socio-economic background of the residents. Specifically, a set of 17 social groups, called ACRON groups, was formed out of the total number of households. Each of these groups is characterized by a set of 825 socio-economic features

clustered in 84 subcategories and 15 main categories. For our evaluation the year 2013 (1st of January 2013 – 31st of December 2013) was used, since year 2012 has several gaps in the measurements, using 50 households per ACRON group, thus a total of 700 households. Furthermore, we excluded ACRON-{B, K, M} as they have missing samples in the selected time interval. The average properties of the 50 households of each ACRON group for the year 2013 are tabulated in Table 1.

TABLE 1. List of Average Properties From the Evaluated ACRON Groups Form the Smart Meters in London Database [45]. The Features of Each ACRON-X Dataset Consist of the Average of 50 Households From the Year 2013.

Dataset	Energy (kWh)	Avg. # People	Avg. Age	Avg. Income (tsd)	Avg. Beds	Avg. Value (tsd)
ACRON-A	4215	3.4	42.3	195	5.2	1321
ACRON-C	4772	2.7	46.5	117	3.9	599
ACRON-D	5200	3.0	32.7	148	3.1	1163
ACRON-E	4251	3.1	32.6	126	3.2	606
ACRON-F	3207	2.8	43.8	103	3.8	425
ACRON-G	3614	3.2	39.2	118	3.8	449
ACRON-H	3671	3.2	38.7	106	3.7	414
ACRON-I	3785	2.2	51.4	75	2.8	401
ACRON-J	3743	2.9	33.9	107	3.2	396
ACRON-L	3208	3.1	36.2	81	3.1	294
ACRON-N	3203	2.2	43.3	46	1.8	270
ACRON-O	2966	2.7	34.0	71	2.4	331
ACRON-P	2290	3.6	30.5	65	2.8	362
ACRON-Q	2671	2.6	33.7	46	1.9	312

As can be seen in Table 1 the ACRON groups cover a wide spectrum of different household characteristics with significant variations in average energy consumption, different number of residents, average age of residents, etc., thus making it suitable for training the proposed LSTM-based architecture using inter-household energy data and socio-economic information.

B. PREDICTOR PARAMETERS

For the regression stage a LSTM model was used, with the architecture of the LSTM being illustrated in Fig. 5, similar as in [46]. The free parameters of the LSTM, namely the number of layers and the number of nodes per layer were optimized after grid search on a bootstrap subset from the SMinL database, using only the energy consumption data of each target house. The free parameters optimization of the LSTM model with respect to the mean absolute error (see Eq. 17) are shown in Table 2.

As can be seen in Table 2 the optimal model consists of two layers with 16 nodes per layer. The state activation function of all LSTM layers is the hyperbolic tangent (tanh).

C. STORAGE PARAMETERS

For the storage modelling described in Section II-C and the storage optimization described in Section III-B the following parameters have been used. We adopted the charging

TABLE 2. Parameter Optimization Results in Terms of MAE (%) for the Proposed LSTM Model for Different Numbers of Layers and Nodes Evaluated on a Bootstrap Dataset of the Smart Meters in London Database [45].

LSTM Nodes	2	4	8	16	32	64	128	256
1	4.89	4.89	4.92	4.89	5.12	4.94	4.90	5.51
2	4.98	5.03	5.10	**4.49**	4.85	5.58	5.07	6.31
3	5.36	5.00	5.85	5.52	5.67	5.85	5.51	5.45
4	5.40	5.26	4.91	5.48	5.06	5.23	5.26	5.71

TABLE 3. Parameters Used for Storage Optimization are Based on the Tesla Home Storage System (PowerWall) as well as Previous Publications [3], [16], [42]. Note That c^*_{init} Refers to the Initial Capacity for the First Day of Evaluation and That the Charging Efficiency of the Tesla Home Storage was Split Equally Between Charging and Discharging Similar as in [16].

Parameter	REF	Variable	Value
charging efficiency	[47]	η^+	0.95
discharging efficiency	[47]	η^-	0.95
maximum charging power	[47]	ρ^+	5.0 kW
maximum discharging power	[47]	ρ^-	-7.0 kWh
self-discharge rate	[16]	λ	10^{-3}
fading constant	[42]	μ_c	10^{-5}
maximum capacity	[3]	c_{max}	64.5 TWh
initial capacity	-	c^*_{init}	$0.25\,c_{max}$
CCCV capacity	[3]	C^*	$0.7 c_{max}$
minimum capacity	[3]	c_{min}	0 TWh

and discharging efficiency parameters (η^+ and η^-) of the Tesla Powerwall 2 with the overall efficiency being equal to 90 % [1]. Furthermore, it was assumed that the charging and discharging efficiency account to equal parts to the overall efficiency. All storage parameters are tabulated in Table 3.

Specifically, the maximum capacity c_{max} was determined such that Eq. 11 can be minimized for the community of households (Section IV-A) as described in [3] and shown in Eq. 16.

$$c_{max} = max\{\int_T P(t) - \overline{P}dt\} - min\{\int_T P(t) - \overline{P}dt\} \quad (16)$$

As tabulated in Table 3 the maximum capacity needed to minimize the grid distortions of the 700 evaluated households are 64.5 TWh, thus 92.1 kWh storage per household being equal to approximately 7 Tesla Powerwall storages. As Tesla Powerwall storages are freely configurable up to 10 storage elements this is a realistic scenario for our evaluation.

D. EVALUATED SCENARIOS

Three different experimental protocols for load prediction and five different experimental protocols for storage optimization were designed. In detail, the load prediction scenarios are the baseline (BL), where a predictor is modelled for every house as described in Eq. 8, the interhousehold (IH), where the predictor is considering neighbouring houses of the community as in Eq. 9 and the social (SO) one considering also social information as described in Eq. 10. Furthermore,

TABLE 4. Four Experimental Protocols With According Storage Sizes (*C*) and Number of Step Ahead Predictions (*W*).

#-Protocol	C	W
1	0	-
2	C_{max}	-
3	$0 < C < C_{max}$	0
4	$0 < C < C_{max}$	$1 \leq w \leq 48$
5	$0 < C < C_{max}$	∞

for the storage optimization five different scenarios, for different sizes of storages and different numbers of ahead predictions *W* have been considered. The experimental protocols are tabulated in Table 4.

In detail protocol #1 is considered as baseline system with no storage installed and thus no optimization applied. Protocol #2 is the ideal case of optimization as in Eq. 12. Protocol #3 is the case of a finite storage without optimization through ahead prediction as in Eq. 13. Protocol #4 is the proposed optimization as in Eq. 15 for different storage sizes and numbers of ahead predictions. Protocol #5 is an ideal case assuming perfect knowledge of future energy consumption, thus without forecasting errors.

V. EXPERIMENTAL RESULTS

The architecture presented in Section II with the optimizations presented in Section III was evaluated according to the experimental setup described in Section IV. Specifically, the performance of the predictor is presented in Section V-A and the load optimization and its influences on the grid distortions are presented in Section V-B.

A. LOAD PREDICTION

The performance of the predictor was evaluated in terms of Mean Absolute Error (MAE), i.e.:

$$MAE = \frac{1}{M} \sum_{m=1}^{M} \frac{\sum_{t=1}^{T} |p_m^t - \hat{p}_m^t|}{T} \qquad (17)$$

where $\hat{p}_m$ is the predicted energy value, *M* is the total number of households and *T* the number of frames. The results for the three different experimental protocols and $W = 48$ samples ahead prediction are illustrated in Fig. 7.

As can be seen in Fig. 7 the IH and SO protocols significantly outperform the baseline system. In detail, for step ahead greater than 40 samples (20 h) the prediction error of the baseline system increases to 5 %, while the IH and SO protocols retain the error below 2 %. This indicates the influence of inter household information and socio-economic information in load demand prediction. Especially, utilizing the energy consumption data of the community of households leads to a significant reduction in forecasting errors (BL protocol vs. IH protocol) which is probably owed to the common energy consumption patterns within households in the same neighbourhood, i.e. there might be temporal shifts between households with different age structure etc., as discussed in Section III-A.
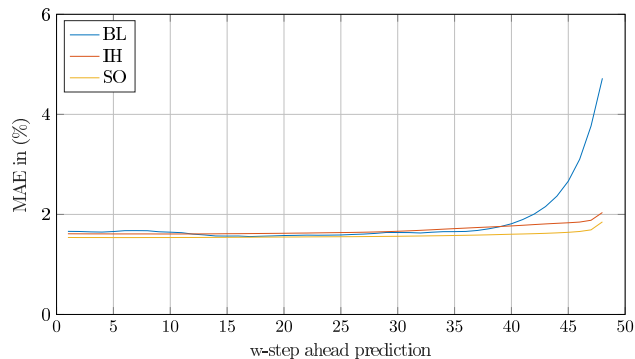

FIGURE 7. Load predictions errors in terms of MAE (%) for different number of steps ahead predictions and different load prediction scenarios: baseline (BL), inter household (IH) and socio-economic (SO), using the load prediction setups from Section III-A.

B. GRID DISTORTION

The performance of the storage optimization was evaluated in terms of peak to average value of the grid power P_G, i.e.:

$$PAR = \sum_T \frac{max(P_G^\tau)}{\sum_{w \in W} P_G^\tau} \qquad (18)$$

where P_G^τ is the grid power of the τth frame and *T* is the number of all frames. The grid distortion for both ideal and real storage models as well as for experimental protocols #1 – #5 are shown in Fig. 8 and Fig. 9.
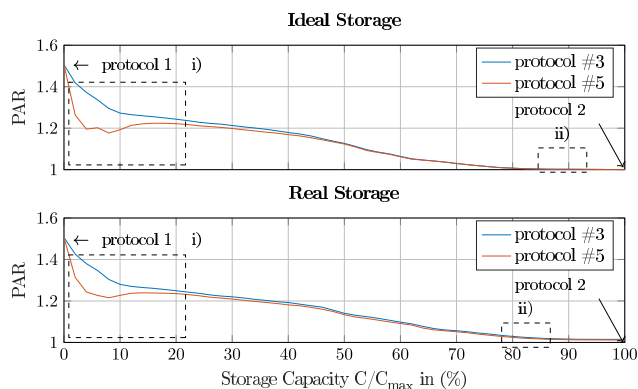

FIGURE 8. Storage optimization without consideration of forecasting errors for ideal storage and real storage models in terms of PAR. In detail, protocol #1 shows distortions without utilizing a storage, protocol #2 considers a storage size large enough to compensate all distortions, protocol #3 illustrates the distortions without any optimization and protocol #5 illustrates the distortions for the proposed optimization in Eq. 15.

As can be seen in Fig. 8 experimental protocol #1 and #2 are independent of the predictor and optimization as with $C = 0$ there is no possible optimization and with $C = c_{max}$ distortion is zero by definition. It is noted, that the ideal storage is reaching zero distortions before the real storage, which is due to the losses of the real storage as described in Section II-C. Furthermore, protocol #3 illustrates the upper boundary for distortions for a specific storage capacity *C* without any optimization and is thus considered as baseline system. Specifically, protocol #5 shows the reduced distortions for a real and ideal storage model without consideration
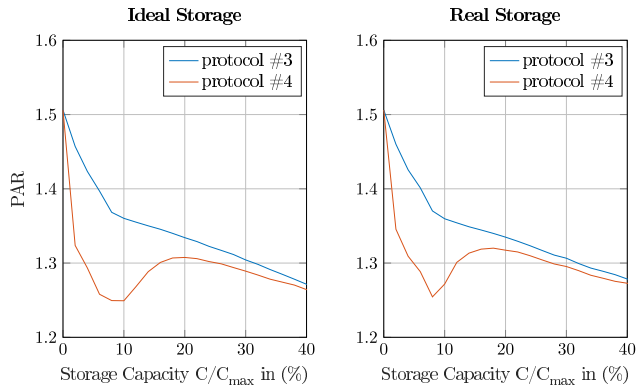
FIGURE 9. Storage optimization with consideration of forecasting errors for ideal storage and real storage models in terms of PAR. In detail, protocol #3 illustrates the reference distortions without utilizing any optimization while protocol #4 illustrates the distortions of the proposed optimizations from Eq. 15 under considerations of the IHS load forecasting protocols as described in Section III-A.

FIGURE 10. Comparison of storage optimization between DSM approach in [16] and the proposed methods with (protocol #4) and without (protocol #5) consideration of forecasting errors.

of forecasting errors. It can be seen that, compared to the baseline system, the largest reductions in grid distortions are achieved within 5-10 % (4.6-8.2 kWh) of the maximum storage capacity as illustrated in area i), which is in line with the work of [1] reporting optimal storage sizes of 5 kWh per household. Specifically, the maximum distortion reduction of protocol #5 is achieved for $C = 8$ % leading to reductions of 12.9 % and 9.9 % for ideal and real storage respectively. Additionally, protocol #4 considering forecasting errors, is shown in Fig. 9.

As shown in Fig. 9 the approach considering load forecasting errors is achieving maximum distortion reduction for $C = 8$ % leading to reductions of 10.0 % and 8.4 % for ideal and real storages, respectively. Compared to the approach without forecasting errors the approach performs 2.5 - 2.9 % worse, which is roughly in the order of the forecasting error as illustrated in Fig. 7.

In order to compare the proposed optimization, the work of Pilz *et al.* utilizing a dynamic game approach, is used for comparison [16]. Specifically, the work in [16] considers protocols with and without forecasting errors as in the proposed approach and uses exactly one year of data while using the same performance metric. Conversely, a different dataset was used utilizing only 25 households with a maximum storage size of 13.5 kWh per household and a variable participation of household in the optimization approach of [16]. Therefore, to assure fair comparison we have recalculated the results using the database [48] and the households as used in [16]. The results are illustrated in Fig. 10.

As illustrated in Fig. 10 the proposed approach leads to equal distortions for maximum storage utilization for both setups with and without consideration of forecasting error. Additionally, distortions are equal without storage utilization by definition.

Conversely, for intermediate storage sizes the proposed method results in minimal grid distortions as described in Section III-B further reducing distortions up-to 10.7 % and
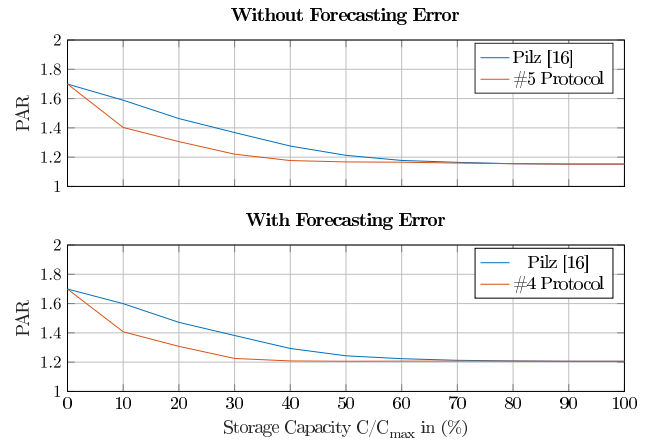
12.1 % for setups with and without consideration of forecasting errors respectively. However, it has to be mentioned that the optimization goal of the DSM scheme in [16] is optimization of the consumer households, thus considers energy pricing, whereas the proposed approach optimizes grid distortions. Therefore, each approach is optimal towards its optimization objective.

VI. DISCUSSION

Further to the presented experimental results in Section V an extended discussion for real world implementation of the proposed architecture is needed. Especially, two different aspect must be considered. First, while the above evaluations have only considered the generation side and specifically the reduction of grid distortions also the consumer side and especially the cost per consumer for a shared energy system must be considered. For the purpose of cost estimation previous articles have proposed different cost functions, i.e. two-step linear functions as described in [49] with different slops or quadratic cost functions [16], [49]. A quadratic cost function as used in [49] is described in Eq. 19:

$$C(E_d) = c_2 E_d + c_1 E_d + c_0 \qquad (19)$$

where $C(E_d)$ describes the dynamic cost depending on the daily energy consumption E_d and $c_2 > 0$, $c_1 \geq 0$ and $c_0 \geq 0$ are a set of hyper-parameters describing the shape of the cost function. In detail c_2 and c_1 define the slope of the quadratic function and thus the dynamic price change depending on the daily energy consumption, while c_0 is an offset parameter and can be seen as a daily fee for being part of a community of consumer households having a shared storage. Therefore, the savings of a consumer being part of a community model with shared storage then depend on the values of c_2, c_1 and c_0, i.e. the questions if it is profitable to pay a small daily fee for having a smaller increase in the cost function compared to having no fixed daily fee while having strongly increasing energy costs. However, numerical estimation of the values c_2, c_1 and c_0 is difficult as many

parameters must be taken into consideration, i.e. initial cost of the storage, cost of wiring and transmission, costs for building accurate load forecasting models, etc., which is outside the scope of this article. Second, as shown in the experimental results the proposed optimizations require data collection from several consumer households, i.e. for building the load prediction model with inter-household connections, as well as socio-economic information. As such information might be privacy sensitive, especially socio-economic information might include properties like residents' age, number of residents per household, etc., evaluations can be performed if users are willing to share such information in return for reduced energy costs or participation in the usage of a shared community energy storage unit. In detail, the acceptance of consumers does significantly influence the ability of real world implementation as a community of households should be in relatively close proximity to the shared energy storage.

VII. CONCLUSION

In this article an storage optimization for a community of households was presented in order to reduce grid distortions. Specifically, the socio-economic information of the community was utilized to improve the quality of the load predictor, and the enhanced prediction results were utilized to reduce the grid distortions using a non-linear convex optimization approach. The proposed methodology was evaluated on the Smart Meters in London database, showing accuracy improvements of up to 3% in terms of absolute MAE improvement for the load prediction and 12.9% reductions of grid distortions for a community of household utilizing one common storage. In detail, it was shown that the proposed optimization procedure leads to minimal grid distortions for an arbitrary storage size and load of a community of households. Specifically, it was shown that the largest performance improvements have been achieved when utilizing 4.6-8.2 kWh of storage per household. Based on the results of utilizing a shared storage in combination with a community based load prediction the following two topics should be investigated in future research. First, a cost function evaluation considering also the cost of having one common load predictor compared to having a single load predictor for each household. Second, investigation of the willingness of consumers to share socio-economic information with the smart-grid and/or utility company in in order to reduce energy bills by utilizing a common energy storage unit. We deem the proposed methodology can result in less grid distortion, which in turn can result in more stable and cost-efficient utility grids, both for the benefit of the provider and the consumer.

REFERENCES

[1] M. Pilz and L. Al-Fagih, "Selfish energy sharing in prosumer communities: A demand-side management concept," in *Proc. IEEE Int. Conf. Commun., Control, Comput. Technol. Smart Grids (SmartGridComm)*, Piscataway, NJ, USA, Oct. 2019, pp. 1–6.
[2] N. L. Panwar, S. C. Kaushik, and S. Kothari, "Role of renewable energy sources in environmental protection: A review," *Renew. Sustain. Energy Rev.*, vol. 15, no. 3, pp. 1513–1524, Apr. 2011.
[3] H.-W. Sinn, "Buffering volatility: A study on the limits of Germany's energy revolution," *Eur. Econ. Rev.*, vol. 99, pp. 130–150, Oct. 2017.
[4] C. Dinesh, S. Makonin, and I. V. Bajic, "Residential power forecasting using load identification and graph spectral clustering," *IEEE Trans. Circuits Syst. II, Exp. Briefs*, vol. 66, no. 11, pp. 1900–1904, Nov. 2019.
[5] C. Deb, F. Zhang, J. Yang, S. E. Lee, and K. W. Shah, "A review on time series forecasting techniques for building energy consumption," *Renew. Sustain. Energy Rev.*, vol. 74, pp. 902–924, Jul. 2017.
[6] P. A. Schirmer, I. Mporas, and M. Paraskevas, "Evaluation of regression algorithms and features on the energy disaggregation task," in *Proc. 10th Int. Conf. Inf., Intell., Syst. Appl. (IISA)*, Jul. 2019, pp. 1–4.
[7] W. Wichakool, A.-T. Avestruz, R. W. Cox, and S. B. Leeb, "Modeling and estimating current harmonics of variable electronic loads," *IEEE Trans. Power Electron.*, vol. 24, no. 12, pp. 2803–2811, Dec. 2009.
[8] K. Amasyali and N. M. El-Gohary, "A review of data-driven building energy consumption prediction studies," *Renew. Sustain. Energy Rev.*, vol. 81, pp. 1192–1205, Jan. 2018.
[9] H. Cai, S. Shen, Q. Lin, X. Li, and H. Xiao, "Predicting the energy consumption of residential buildings for regional electricity supply-side and demand-side management," *IEEE Access*, vol. 7, pp. 30386–30397, 2019.
[10] P. Lusis, K. R. Khalilpour, L. Andrew, and A. Liebman, "Short-term residential load forecasting: Impact of calendar effects and forecast granularity," *Appl. Energy*, vol. 205, pp. 654–669, Nov. 2017.
[11] P. Vrablecová, A. Bou Ezzeddine, V. Rozinajová, S. Šárik, and A. K. Sangaiah, "Smart grid load forecasting using online support vector regression," *Comput. Electr. Eng.*, vol. 65, pp. 102–117, Jan. 2018.
[12] T.-Y. Kim and S.-B. Cho, "Predicting residential energy consumption using CNN-LSTM neural networks," *Energy*, vol. 182, pp. 72–81, Sep. 2019.
[13] M.-N. Heris, M. A. Mirzaei, S. Asadi, B. Mohammadi-Ivatloo, K. Zare, H. Jebelli, and M. Marzband, "Evaluation of hydrogen storage technology in risk-constrained stochastic scheduling of multi-carrier energy systems considering power, gas and heating network constraints," *Int. J. Hydrogen Energy*, vol. 45, no. 55, pp. 30129–30141, Nov. 2020.
[14] M. A. Mirzaei, M. Nazari-Heris, K. Zare, B. Mohammadi-Ivatloo, M. Marzband, S. Asadi, and A. Anvari-Moghaddam, "Evaluating the impact of multi-carrier energy storage systems in optimal operation of integrated electricity, gas and district heating networks," *Appl. Thermal Eng.*, vol. 176, Jul. 2020, Art. no. 115413.
[15] M. Nazari-Heris, M. A. Mirzaei, B. Mohammadi-Ivatloo, M. Marzband, and S. Asadi, "Economic-environmental effect of power to gas technology in coupled electricity and gas systems with price-responsive shiftable loads," *J. Cleaner Prod.*, vol. 244, Jan. 2020, Art. no. 118769.
[16] M. Pilz and L. Al-Fagih, "A dynamic game approach for demand-side management: Scheduling energy storage with forecasting errors," *Dyn. Games Appl.*, vol. 10, pp. 897–929, 2020, doi: 10.1007/s13235-019-00309-z.
[17] H. K. Nguyen, J. B. Song, and Z. Han, "Distributed demand side management with energy storage in smart grid," *IEEE Trans. Parallel Distrib. Syst.*, vol. 26, no. 12, pp. 3346–3357, Dec. 2015.
[18] K. Yuasa, I. Omura, M. Ueshima, and T. Babasaki, "Power energy cost reduction effects by applying optimized long-term storage battery operation strategy," in *Proc. 8th Int. Conf. Renew. Energy Res. Appl. (ICRERA)*, Piscataway, NJ, USA, Nov. 2019, pp. 107–112.
[19] A. G. N. Madhuranga and I. A. Premaratne, "Energy storage battery bank system to reduce peak demand for domestic consumers," in *Proc. Int. Conf. Comput., Commun. Electron. (Comptelix)*, I. Staff, Ed., Piscataway, NJ, USA, Jul. 2017, pp. 648–653.
[20] M. Pilz, L. Al-Fagih, and E. Pfluegel, "Energy storage scheduling with an advanced battery model: A game–theoretic approach," *Inventions*, vol. 2, no. 4, p. 30, 2017.
[21] N. Huang, W. Wang, S. Wang, J. Wang, G. Cai, and L. Zhang, "Incorporating load fluctuation in feature importance profile clustering for day-ahead aggregated residential load forecasting," *IEEE Access*, vol. 8, pp. 25198–25209, 2020.
[22] C. Ju, P. Wang, L. Goel, and Y. Xu, "A two-layer energy management system for microgrids with hybrid energy storage considering degradation costs," *IEEE Trans. Smart Grid*, vol. 9, no. 6, pp. 6047–6057, Nov. 2018.
[23] K. Rahbar, J. Xu, and R. Zhang, "Real-time energy storage management for renewable integration in microgrid: An off-line optimization approach," *IEEE Trans. Smart Grid*, vol. 6, no. 1, pp. 124–134, Jan. 2015.

[24] B.-R. Ke, T.-T. Ku, Y.-L. Ke, C.-Y. Chuang, and H.-Z. Chen, "Sizing the battery energy storage system on a university campus with prediction of load and photovoltaic generation," *IEEE Trans. Ind. Appl.*, vol. 52, no. 2, pp. 1136–1147, Mar./Apr. 2016.

[25] J. Li, H. You, J. Qi, M. Kong, S. Zhang, and H. Zhang, "Stratified optimization strategy used for restoration with photovoltaic-battery energy storage systems as black-start resources," *IEEE Access*, vol. 7, pp. 127339–127352, 2019.

[26] Y. Wang, X. Lin, and M. Pedram, "A near-optimal model-based control algorithm for households equipped with residential photovoltaic power generation and energy storage systems," *IEEE Trans. Sustain. Energy*, vol. 7, no. 1, pp. 77–86, Jan. 2016.

[27] M. S. Rahman, M. J. Hossain, J. Lu, F. H. M. Rafi, and S. Mishra, "A vehicle-to-microgrid framework with optimization-incorporated distributed EV coordination for a commercial neighborhood," *IEEE Trans. Ind. Informat.*, vol. 16, no. 3, pp. 1788–1798, Mar. 2020.

[28] O. Erdinc, N. G. Paterakis, T. D. P. Mendes, A. G. Bakirtzis, and J. P. S. Catalao, "Smart household operation considering bi-directional EV and ESS utilization by real-time pricing-based DR," *IEEE Trans. Smart Grid*, vol. 6, no. 3, pp. 1281–1291, May 2015.

[29] F. Hafiz, P. Fajri, and I. Husain, "Load regulation of a smart household with PV-storage and electric vehicle by dynamic programming successive algorithm technique," in *Proc. IEEE Power Energy Soc. Gen. Meeting (PESGM)*, I. Staff, Ed., Piscataway, NJ, USA, Jul. 2016, pp. 1–5.

[30] L. Chandra and S. Chanana, "Energy management of smart homes with energy storage, rooftop PV and electric vehicle," in *Proc. IEEE Int. Students' Conf. Electr., Electron. Comput. Sci. (SCEECS)*, Feb. 2018, pp. 1–6.

[31] H. Gong, O. Akeyo, V. Rallabandi, and D. M. Ionel, "Real time operation of smart homes with PV and battery systems under variable electricity rate schedules and transactive power flow," in *Proc. 7th Int. Conf. Renew. Energy Res. Appl. (ICRERA)*, I. Staff, Ed., Piscataway, NJ, USA, Oct. 2018, pp. 1392–1395.

[32] M. M. Iqbal, I. A. Sajjad, M. F. N. Khan, R. Liaqat, M. A. Shah, and H. A. Muqeet, "Energy management in smart homes with pv generation, energy storage and home to grid energy exchange," in *Proc. 1st Int. Conf. Electr., Commun. Comput. Eng. (ICECCE)*, Piscataway, NJ, USA, 2019, pp. 1–7.

[33] S. Baldi, A. Karagevrekis, I. T. Michailidis, and E. B. Kosmatopoulos, "Joint energy demand and thermal comfort optimization in photovoltaic-equipped interconnected microgrids," *Energy Convers. Manage.*, vol. 101, pp. 352–363, Sep. 2015.

[34] C. D. Korkas, S. Baldi, I. Michailidis, and E. B. Kosmatopoulos, "Occupancy-based demand response and thermal comfort optimization in microgrids with renewable energy sources and energy storage," *Appl. Energy*, vol. 163, pp. 93–104, Feb. 2016.

[35] H. R. Gholinejad, A. Loni, J. Adabi, and M. Marzband, "A hierarchical energy management system for multiple home energy hubs in neighborhood grids," *J. Building Eng.*, vol. 28, Mar. 2020, Art. no. 101028.

[36] H. Ganjeh Ganjehlou, H. Niaei, A. Jafari, D. O. Aroko, M. Marzband, and T. Fernando, "A novel techno-economic multi-level optimization in home-microgrids with coalition formation capability," *Sustain. Cities Soc.*, vol. 60, Sep. 2020, Art. no. 102241.

[37] M. Jadidbonab, B. Mohammadi-Ivatloo, M. Marzband, and P. Siano, "Short-term self-scheduling of virtual energy hub plant within thermal energy market," *IEEE Trans. Ind. Electron.*, vol. 68, no. 4, pp. 3124–3136, Apr. 2021.

[38] A. Al-Haj Hussein and I. Batarseh, "A review of charging algorithms for nickel and lithium battery chargers," *IEEE Trans. Veh. Technol.*, vol. 60, no. 3, pp. 830–838, Mar. 2011.

[39] A. Jossen and W. Weydanz, *Moderne Akkumulatoren Richtig Einsetzen*, 1st ed. Neusäß, Germany: Ubooks-Verlag, 2006.

[40] R. Yazami and Y. Reynier, "Mechanism of self-discharge in graphite–lithium anode," *Electrochimica Acta*, vol. 47, no. 8, pp. 1217–1223, Feb. 2002.

[41] J. Vetter, P. Novák, M. R. Wagner, C. Veit, K.-C. Möller, J. O. Besenhard, M. Winter, M. Wohlfahrt-Mehrens, C. Vogler, and A. Hammouche, "Ageing mechanisms in lithium-ion batteries," *J. Power Sources*, vol. 147, nos. 1–2, pp. 269–281, 2005.

[42] L. Ahmadi, M. Fowler, S. B. Young, R. A. Fraser, B. Gaffney, and S. B. Walker, "Energy efficiency of li-ion battery packs re-used in stationary power applications," *Sustain. Energy Technol. Assessments*, vol. 8, pp. 9–17, Dec. 2014.

[43] P. A. Schirmer, C. Geiger, and I. Mporas, "Residential energy consumption prediction using inter-household energy data and socioeconomic information," in *Proc. 28th Eur. Signal Process. Conf. (EUSIPCO)*, Jan. 2021, pp. 1595–1599.

[44] P. A. Schirmer, I. Mporas, and I. Potamitis, "Evaluation of regression algorithms in residential energy consumption prediction," in *Proc. 3rd Eur. Conf. Electr. Eng. Comput. Sci. (EECS)*, Dec. 2019, pp. 22–25.

[45] *SmartMeter Energy Consumption Data in London Households*. [Online]. Available: https://www.kaggle.com/jeanmidev/smart-meters-in-london/metadata

[46] L. Mauch and B. Yang, "A new approach for supervised power disaggregation by using a deep recurrent LSTM network," in *Proc. IEEE Global Conf. Signal Inf. Process. (GlobalSIP)*, Piscataway, NJ, USA, Dec. 2015, pp. 63–67.

[47] *Tesla Powerwall 2*, Tesla, San Carlos, CA, USA, 2017.

[48] *Commerical and Residential Hourly Load Profiles for All Tmy3 Locations in the United States*, U.S. Dept. Energy, 2013. [Online]. Available: https://openei.org/doe-opendata/dataset/commercial-and-residential-hourly-load-profiles-for-all-tmy3-locations-in-the-united-states

[49] A.-H. Mohsenian-Rad, V. W. S. Wong, J. Jatskevich, R. Schober, and A. Leon-Garcia, "Autonomous demand-side management based on game-theoretic energy consumption scheduling for the future smart grid," *IEEE Trans. Smart Grid*, vol. 1, no. 3, pp. 320–331, Dec. 2010.

PASCAL A. SCHIRMER received the B.Eng. degree in electrical engineering from the University of Applied Sciences, Esslingen, Germany, in 2018. He is currently pursuing the Ph.D. degree in electrical appliances modeling and energy disaggregation with the University of Hertfordshire. Since 2018, he has been a Research Associate with the School of Engineering and Computer Science, University of Hertfordshire. His research interests include electric drives, power electronics, and life-time evaluation.

CHRISTIAN GEIGER received the B.Eng. degree in electrical engineering from the University of Applied Sciences, Esslingen, Germany, in 2018, and the M.Sc. degree in electrical engineering, with focus on automation and robotics, from the Technical University of Munich (TUM), where he is currently pursuing the Ph.D. degree. Since 2019, he has been doing research on the fabrication of all-solid-state batteries with the Institute for Machine Tools and Industrial Management (iwb), TUM.

IOSIF MPORAS received the Diploma (5-years) degree in electrical and computer engineering and the Ph.D. degree from the University of Patras, Greece, in 2004 and 2009, respectively. From 2010 to 2016, he was an Adjunct Assistant Professor with the Technological Educational Institute of Western Greece. From 2009 to 2016, he was a Postdoctoral Researcher with the University of Patras. Since 2016, he has been a Senior Lecturer in information engineering with the University of Hertfordshire, U.K. He has participated in more than 10 EU-funded Research and Development projects as a researcher, a senior researcher, and a principal investigator. He has published more than 100 articles in international journals and conferences cited more than 1000 times. His research interests include the applications of signal processing and machine learning. He was the General Chair of the Joint SPECOM/ICR 2017 Conference and the Technical Chair of the ICESF 2020 Conference. He serves as reviewer for grant applications and international journals, and as a programme committee member in international conferences.

• • •